J Vis (2022) 25:501–509
https://doi.org/10.1007/s12650-021-00816-5

REGULAR PAPER

Idera Lawal · Pankaj Rohilla · Jeremy Marston

Visualization of drug delivery via tattooing: effect of needle reciprocating frequency and fluid properties

Received: 5 May 2021 / Revised: 26 October 2021 / Accepted: 28 October 2021 / Published online: 14 January 2022

Abstract Tattooing is a commonplace practice among the general populace in which ink is deposited within dermal tissue. Typically, an array of needles punctures the skin which facilitates the delivery of a fluid into the dermis. Although, a few studies in the past have investigated the potential of tattooing as an intradermal (ID) drug injection technique, an understanding of the fluid dynamics involved in the delivery of fluid into skin is still lacking. Herein, we sought to provide insight into the process via an *in vitro* study. We utilize a five needle flat array (5F) with a tattoo machine to inject fluids into gelatin gels with modulus $\sim$ 15 kPa. High-speed imaging was used to visualize the injection process and estimate the amount of fluid delivered after each injection up to the 50th injection. We investigate the role of reciprocating frequency ($f = O(10 - 100)$ Hz) and physical properties of the fluids on the volume infused ($V_o \sim O(100)$ nL) after injection. We find that V_o is only slightly dependent on f, however volume delivered increases with decreasing viscosity. In addition, we illustrate the physical mechanism of infusion during tattooing, which has not been reported. An understanding of the injection process via tattooing can be useful in the development of ID tattoo injectors as drug delivery devices.

Keywords Tattooing · Drug delivery · Fluid dynamics · Capillary imbibition

1 Introduction

The tattooing technique reportedly dates back to the Neolithic period from ancient artifacts discovered by archaeologists (Friedman et al. 2018), but only to the fourth millennium BC based on tattoos found on mummified human skin (Petersen and Roth 2016). The artifacts and skin samples suggest that the tattoos were either intended for cosmetic aesthetic or for the concealing of body defects such as baldness, scars and the appearance of a nipple after mastectomy (Kluger and Koljonen 2012).

To date, tattooing is widely practiced and the number of people with at least one tattoo has seen major increase worldwide (Petersen and Roth 2016). An estimated 1 in 3 Americans have at least one tattoo with other countries like Italy or Sweden having even higher statistics (Sato et al. 1999). Several studies have shown that skin type and individual innate immune system make up are key factors in whether the tattoo results in allergic reactions; these factors also determine how much of the ink is injected (20% - 50% effective volume) (Jang et al. 2009). Therefore, from population magnitude alone, the process poses

Supplementary Information The online version contains supplementary material available at https://doi.org/10.1007/s12650-021-00816-5.

I. Lawal · P. Rohilla · J. Marston (✉)
Department of Chemical Engineering, Texas Tech University, Lubbock, TX 79409, USA
E-mail: jeremy.marston@ttu.edu

motivation for scientific and technological inquiry into abating health risk and improving patient compliance.

The tattooing procedure involves the invasive repeated puncture by 200-350 micron sized needles, intradermally (0.5-2 mm depth). This effectively injures the topmost part of the skin as needle movement facilitates influx of ink into the injury site with each successive puncture. Needles used vary in both number and conformation, and the amount of ink delivered is dependent on ink makeup, skin properties and the depth and density of punctures (punctures per unit area). Tattoo inks are generally colorants made of metallic salts which are suspended in a carrier solution along with binders, surfactants and other additives (Jang et al. 2009). The specific composition of the inks is kept secret by manufacturers, however because each formulation is tailored to optimum fluid dynamic properties for delivery, rheological behavior suffices for characterization (Sato et al. 1999). The number of needles on each cartridge head usually lies between 1 and 23, and according to professional tattoo artists, the number and conformation of tattoo needle heads directly correlates with how much skin is desired to be covered for the art that is to be portrayed. Larger number of needles are typically used for shading and filling work, whereas smaller number of needles are used for drawing of lines. Likewise in conformation, more tightly packed arrangements (liners) are utilized for drawing definitive lines while more loosely packed sets of needles are used for shading.

After the procedure, the body's immune system kicks into overdrive (from the thousands of micro injuries that just occurred) and responds by; inflammation which is immediately triggered by tissue phagocytes at the scene of injury. These cells release histamines that cause a transient increase in vasodilation and vascular permeability accompanied with the release of cytokines that signal the next phase; influx of monocytes through the blood vessels (aided by vasodilation). Monocytes become macrophages when they reach the site of injury, after which they either consume the deposited ink and traverse to the lymph nodes for excretion or remain in the dermis (a reason for the seemingly permanent nature of tattoos) (Petersen and Roth 2016).

DNA vaccination and some novel therapeutic treatments also involve intradermal delivery. Over the past several decades, DNA vaccination has evolved from volume profligate intramuscular (IM) injections to antigen – sparing intradermal doses that have similar or improved immune responses (Mohammed et al. 2010; Belshe et al. 2004; Bryan et al. 1992; Rohilla and Marston 2020; Weniger and Papania 2013). This fractional dosing involves subjects receiving a single shot of just 20% the full dose. However, challenges such as needle-stick injuries and cross contamination persist. Jet injectors (Mohammed et al. 2010); micro-needle patches (Yuen and Liu 2015); ballistic vaccination methods such as the gene gun (Peng et al. 2010) and epidermal powder immunization (Chen et al. 2003); are examples of needle free alternatives that circumvent such difficulty. Moreover, the delivery of DNA vaccines can also be challenging. It constitutes deeply entangled, high molecular weight suspensions which are highly viscous and shear thinning and thus sensitive to hydrodynamic shear (Lengsfeld and Anchordoquy 2002). For this reason, the needle free jet injector is preferred due to the high shearing that occurs $O(\sim 10^6 s^{-1})$ albeit concerns about high shear degradation have been reported (Lengsfeld and Anchordoquy 2002).

The extent to which the immune system responds has driven several investigations into the efficacy of the tattooing process in intradermal (ID) drug delivery (Jang et al. 2009). Some studies adapt the tattoo machine for even injection into a large area, effectively portioning medication into fractional doses (Quaak et al. 2009). To state a few, Shio et al. (2014) utilize a five needle magnum head for the treatment of cutaneous leishmaniasis (a parasitic disease which causes skin sores) in their study. Each session consisted of a fractional dosage of 12 two-second applications twice everyday for five days, successfully administering approximately 2-5 microlitres of treatment onto the sores to attenuate the effects of the disease. In a similar study, Quaak et al. (2009) conduct in vitro and ex vivo tattooing of plasmid DNA solutions using a nine needle flat head to probe the extent to which their Murine models had antigen expression and T-cell responses. Furthermore, Potthoff et al. (2009) confirmed that in comparison to ID injections, tattoo immunization restrict antigen expression to the topmost layer of the dermis even though expression levels are similar. Therein, an 11 magnum head needle is used for 10 microliter fractional doses. Studies on the tattooing process are not restricted to vaccination and treatment of disease alone. Other work includes probing into the immune response (Gopee et al. 2005) and recovery from tattooing in a bid to illuminate on the toxicology of tattoo inks and pigments. In that study, a 14 magnum needle head is utilized. Interestingly, the basis for which the number and conformation of needles used is not usually reported in these studies.

As far as the physics of the process, very few literature exists that detail the intricacies of the process (Cu et al. 2019; Gálvez et al. 2019) and more rigorous descriptions of the physics behind the tattooing procedure is lacking despite the several reports on the immunological response of the process.

In this study, we use a transparent gelatin gel to understand the injection mechanism via tattooing process. We used DI water and 80% glycerol as Newtonian fluids, and two commercial inks (black and red ink) exhibiting non-Newtonian behavior as fluids to be injected using a tattoo pen equipped with a five needle array in a flat conformation. We compared the volume delivered for different number of repeat injections and varying needle reciprocating frequency.

2 Materials and methods

An atom pen rotary tattoo machine (*Dragonhawk Tattoo Supply, China*) was used. A 12-gauge 5F tattoo needle (*five needles arranged in a flat array*) with each needle having a total length of 10 mm (tapered length ~ 1 mm from the tip) and a diameter of 0.35 mm, was used with the tattoo machine. 5F needles were chosen for this study because they are deemed the most relevant/practical for the tattooing process. This resulting from a nexus of three considerations; its average use in studies (Quaak et al. 2009; Shio et al. 2014), being the default go to for tattoo artists who have to make a trade-off between area of skin covered and the level of pain experienced by the customers (more needles = more covered area per puncture but more pain), and for ease of visualization, other needle conformations prove difficult for a 2D camera recording. The exposure of the needles (length of the needles protruding from the cartridge) is set to $\sim$ 1 mm for all experiments.

In order to simulate a range of rheological profiles for real vaccines, dyed DI water and 80% glycerol (G, *Macron*) were used in addition to the black and red ink pigments (*Mom's Millenium, USA*) as injectates. The reciprocating frequency of needles (46–72 Hz) was varied via voltage control in a range of 3–5 V. Figure 1a shows the schematics of the experimental setup used. Rheological measurements of ink pigments were performed on a DHR-2 rheometer (*TA Instruments, USA*) with a cone and plate geometry (25 mm diameter and 1.992° angle) and at a temperature of 22 ± 1 °C. The flow behavior of ink pigments were measured via flow ramp tests for applied shear rates ranging from 0.001 to 5000 s^{-1}, see results in Fig. 2a. The rheological profiles for black and red ink presented in Fig. 2a were fit to the cross-model (Cross 1965) to get the apparent viscosity as: $\mu_a = \mu_\infty + (\mu_0 - \mu_\infty)/1 + (\lambda\dot{\gamma})^n$, where μ_0 and μ_∞ are first and second Newtonian plateau, λ and n are constants which are obtained by the model fitting. Insertion and retraction velocities with variation in reciprocating frequency of 5F needle array is presented in Fig. 2b. A linear fit yields a relation between the needle array velocity and the reciprocating frequency ($f \in [20\ 200]$) given by, $v = 0.00544f - 0.01247$. Velocity of needle array was estimated to be [0.237, 0.314, 0.379] m/s from this linear fit corresponding to frequency used in the study $f \in [46, 60, 72]$ Hz.

We estimated applied shear rates ($\dot{\gamma} = v_i/h = 2a_m\pi f/D_{needle}$ where a_m is the maximum displacement of the needle) just as in Gálvez et al. (2019) which were on the order of $\sim 10^3\ s^{-1}$ for $v_i \in [0.24\ 0.38]\ m/s$. Estimated apparent viscosity (μ_a) corresponding to these shear rates for black and red inks were ~ 0.042 Pa.*s* and ~ 0.049 Pa.*s*, respectively. Viscosity of DI water and 80% glycerol were used as 8.9×10^{-4} Pa.*s* and 0.084 *Pa.s*, respectively. We used trypan blue (*Sigma-Aldrich*) as a dye in a concentration of 5 mg/ml for DI water and 80% glycerol solution.

A high-speed camera (*Phantom V711, Vision Research Ltd*) was used to capture the motion of the reciprocating needles and injections at a frame rate of 8000 fps with pixel size of 16μm/px (Spatial resolution: 400 x 800). A Nikon micro-nikkor 60 mm lens was used with a 28 mm extension tube. Figure 1b shows the reciprocating motion of the needle with a frequency of 46 Hz corresponding to a voltage of 3 V. Insertion velocity ($v_i = \Delta y_i/\Delta t_i$) and retraction velocity ($v_r = \Delta y_r/\Delta t_r$) were estimated by tracking the needle tip using image processing via a custom MATLAB Script. It is noteworthy that these velocities do not deviate much even inside the substrate.

An in vitro study was conducted to understand the mechanism of drug delivery via tattooing. A $5\%_{w/w}$ of gelatin solution (*from bovine skin – 225 g Bloom, Type B, Sigma–Aldrich*) is selected as the substrate because it has been considered as a good substitute for human tissue (Rohilla and Marston 2019). It was prepared by mixing in water at a temperature of 65 °C while stirring at 650 rpm. The elastic modulus was ~ 15 *kPa* as measured using a spherical indenter of diameter ~ 3 *mm*. Moreover, the elastic modulus of skin tissue lies within the range of 1–30 kPa (Delalleau et al. 2006; Pailler-Mattei et al. 2008) further confirming our choice. Different fluids were injected via tattoo machine with different reciprocating frequencies of the needle array (46, 60 and 72 Hz). To estimate the volume of liquid delivered inside the gel, snapshots of fluid infusion inside the gel were taken after every complete needle retraction, and then

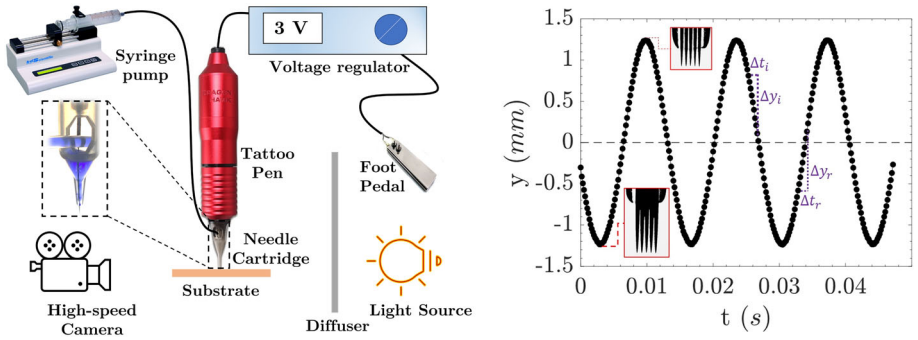

Fig. 1 **a** Schematics of experimental setup (inset shows how ink is fed to the cartridge) and **b** needle displacement frequency of a 5F tattoo needle for a voltage of 3 V

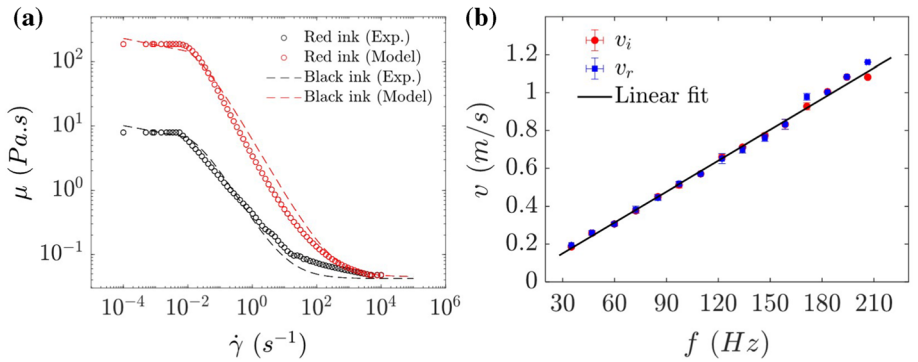

Fig. 2 **a** Rheological measurements for different inks used and **b** insertion and retraction velocities of 5F needle array for different f with a linear fit

analyzed with a MATLAB script to estimate the dimensions of the cavity created by the injection. A cone approximation technique was used in a previous study (Gálvez et al. 2019) which gave erroneous estimation of the injected volume for our study due to the irregular shape of dispersion pattern after injections. Herein, we use a disk approximation (*see supplementary information*) to estimate the injected volume to avoid the overestimation of the injected volume.

3 Results and discussion

3.1 Tattoo injection mechanism

Figure 3 shows schematics and snapshots depicting the salient features of the tattooing process on the gel substrate by a 5F needle array. The puncturing process was observed to occur in four distinct phases for the first injection and for reference, we have termed them; the (*i*) piercing, (*ii*) relaxation, (*iii*) retraction and (*iv*) deposition phases sequentially. Upon actuation, the needles move downward and as they contact the substrate, the piercing phase begins. The needle array coated with a thin film of the fluid used, punctures the gel substrate at an insertion speed of $v_i \in [0.24\ 0.38]$ m/s. The gel surface deforms in a concave shape as the needles move downwards (Fig. 3b: $t = 1.5\ ms$). This continues until the gel surface reaches maximum deformation, after which it begins to relax, pulling back upwards, however needle piercing continues downwards (Fig. 3b: $t = 6\ ms$). The needle reaches a maximum displacement corresponding to a time t_1 (Fig. 3b: $t = 6.9\ ms$) at which motion is briefly halted before moving in the opposite direction with a retraction speed of $v_r \approx v_i$.

As the needles retract, cavities are left behind and they begin to contract (Fig. 3b: $t = 8.1\ ms$), this constitutes the retraction phase. During retraction, these cavities contract due to elastic relaxation forces in the gel matrix (Fig. 3a: $t = t_2$). Simultaneously, the gel surface follows the motion of the needles as a result

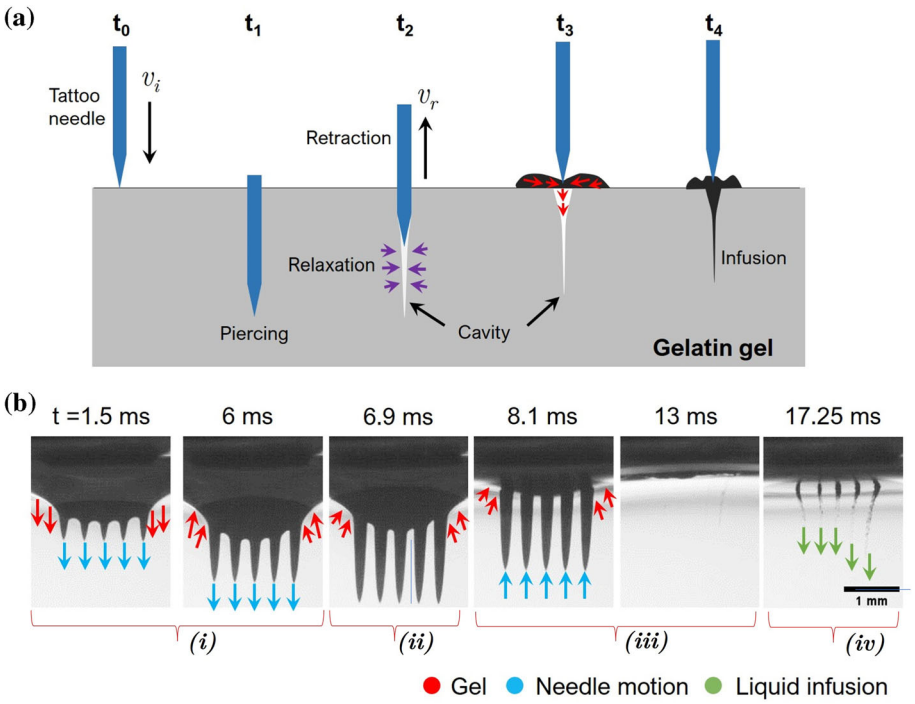

Fig. 3 **a** Schematic representation of hypothesized mechanism for fluid deposition via tattoo injection and **b** Snapshots showing black ink deposition after first injection for $f = 60$ Hz

of adhesion forces between the gel and the needles, and is pulled upwards right before complete retraction. The surface of the gel deforms in a convex shape during the retraction of the needles from the surface (Fig. 3b: $t = 13\ ms$). Complete retraction of the needles leaves cavities open to the surface and exposed to fluid present in the vicinity (Fig. 3a: $t = t_3$). At time t_4, the needles have withdrawn completely from the substrate and fluid infusion begins, fluid on the gel surface is imbibed into the cavities (Fig. 3b: $t = 17.25$). This capillary imbibition can best be described by the wicking experiments in Andersson et al. (2017) ergo it follows that fluid is infused into the substrate at a rate dependent on the dimensions of the cavity formed, wettability of the substrate, and the physical properties of the fluid as described by Eqs. (3) and (11) in Andersson et al. (2017). While a more robust description of the mechanism of this imbibition will be pursued in a subsequent publication, herein we seek a qualitative overview of the tattooing process.

For further insight into the fluid infusion process, we performed injections with bare needles (hereafter referred to as "dry injections") and with needles coated with the red ink. Figure 4 shows this comparison during the first injection. At the incipient stages, piercing and deforming is qualitatively similar, however

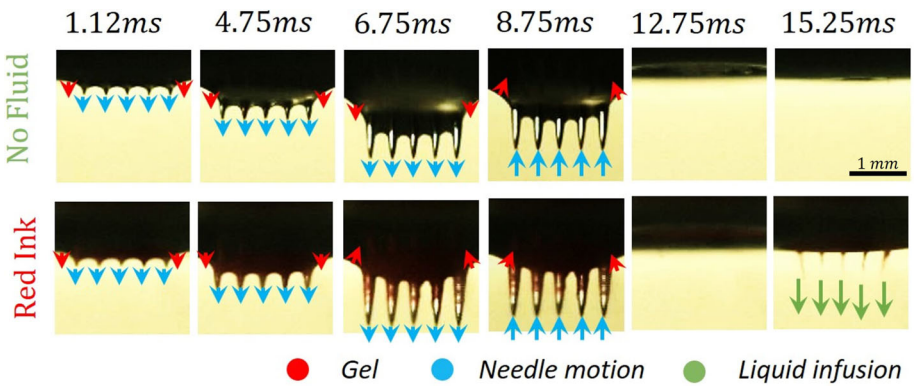

Fig. 4 Image sequence showing the needles puncturing $5\%_{w/w}$ gelatin gel, with and without fluid coating (Only the first cycle is shown to illustrate the effect of lubrication and infusion mechanism)

distinctions become observable in the relaxation phase ($t = 6.75\ ms$). In the case of needles coated with fluid, the gel surface moves upwards earlier as compared to the case of bare needles. The fluid coating minimizes the adhesion between the needle and the gel resulting in earlier relaxation of the gel surface, i.e., the coating fluid 'lubricates' the needle and may promote enhanced penetration compared to dry injection. It should be noted that the cavities were not visible in the case of bare needle injection, but can be seen as fluid infused inside the gel in the case of needles coated with the red ink.

3.2 Viscosity and reciprocating frequency effects

The insights from the dry vs wet injection comparison help us understand that, upon successive injections, the dimensions of the cavity left behind increase. However the needles themselves travel to the same depth after every injection. This can be seen in the top strip of Fig. 5a which shows the needles coated with the red ink at maximum penetration depth after N injections into the gel. It is noteworthy that with increasing N, fluid coating visibly extends to the tip of the needles at $N > 5$. In addition, the cavities formed by the needles were observed to transit from the elastic deformation to plastic deformation. This transition can be observed with the changing shape of the cavities filled with the red ink in the lower strip of Fig. 5a. Thus, the amount of fluid infused (*for the red ink in this case*) increased with the increasing N (Fig. 5a), a phenomenon that has been observed previously (Gálvez et al. 2019). Figure 5b shows the volume of dyed water delivered into the gel with increase in number of injections. Typically, about 50% of the volume was delivered by $N \simeq 10$, whereas it takes 40 more injections to inject the remaining volume.

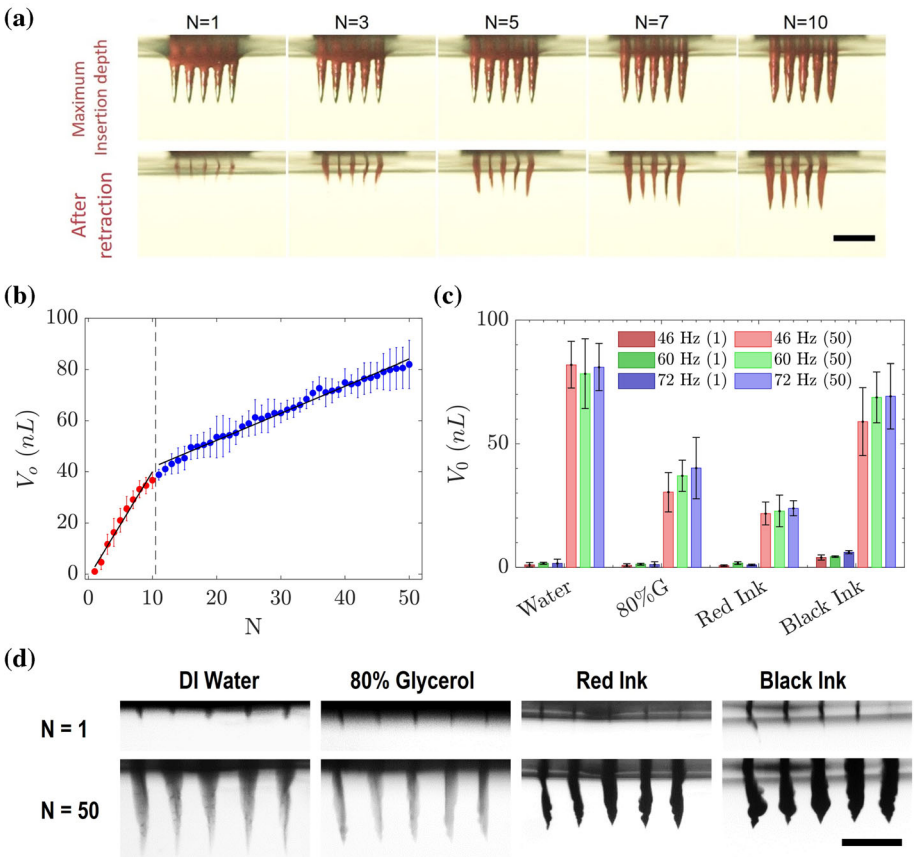

Fig. 5 **a** Image sequence showing amount of ink left in substrate after N injections by the needle array coated with red ink at the maximum insertion depth and after the retraction, $f = 60\ Hz$ (Scale bar represents 1 mm), **b** Typical volume (V_o) distribution over injection number (in this case DI water at $f = 46\ Hz$), **c** Effect of frequency, f on volume infused, V_o for different fluids after first (lighter bars, $N = 1$) and 50^{th} injection (darker bars, $N = 50$), **d** snapshots of ink infusion at 72Hz after initial (top) and final (bottom) injection for all fluids used. Several repeat trials were done for subfigures (b) and (c)

Furthermore we investigate the effect of needle speed by varying reciprocating frequency (f) of the needle array which was controlled by applied voltage. We used f in the range of 46-72 Hz for infusion of two Newtonian (DI water and 80% glycerol) and two non-Newtonian fluids (red and black ink). Figure 5c shows the effect of varying f for different fluids over a range of injections, $N = 1 - 50$.

To screen out viscosity effects, we contrast fluid deposition across all fluids for the first injection, ($N = 1$, lighter shades) and the 50^{th} injection, ($N = 50$, darker shades) as seen in Fig. 5c. At $N = 1$, although the effect is only very slight, volume infused was seen to increase with decreasing viscosity as is evident from the higher values for black ink and water as against red ink and 80% G, i.e., imbibition scales inversely with fluid viscosity.

By the 50^{th} injection, this behavior is magnified, as shown by the stark difference in volume delivered in both Newtonian and non-Newtonian fluids. Volume delivered for water, ($V_{o,DI}$) is nearly double that of 80% glycerol ($V_{80\%G}$), further highlighting the role of viscosity in the fluid infusion process for Newtonian fluids. The tattoo inks (non-Newtonian) however present interesting discourse. The volume delivered for black ink, $V_{o,black}$ is 2.8 times that for red ink, $V_{o,red}$ suggesting that this inverse viscosity relation holds. However, with the earlier assumed shear rate ($\dot{\gamma} \sim 10^3 s^{-1}$), the apparent viscosity of black and red ink are nearly the same. We therefore posit that the fluid imbibition occurs at a rate, v_{imb} which depends on fluid surface tension, σ, fluid viscosity, μ, and opening angle of the cavity, ϕ and scales as Eq. 1, just as in the wicking experiments in Prakash et al. (2008)

$$v_{imb} \sim \frac{\sigma\phi}{\mu} \tag{1}$$

We can then make sense of the results herein. It is noteworthy that ϕ is a parameter that we believe is dependent on the lubrication of the needles, i.e., if the fluid is better at lubricating the needles, the needles more easily pierce the substrate and thus leave behind a more defined cavity. Conversely we may have overestimated shear rates and imbibition may occur at much lower shear rates ($\dot{\gamma} \sim O(10^0 - 10^{-1}\ s^{-1})$) which have an ensuing order of magnitude difference in apparent viscosity ($\mu_{a,black} = 0.5$, $\mu_{a,red} = 5$). In which case, the inverse viscosity relationship is again valid. Nonetheless, it is clear from Fig. 5c that a lower viscosity is preferable with regard to increasing delivery volume.

We performed ANOVA to understand the effect of viscosity and reciprocating frequency on the volume delivered inside the gel. The effect of apparent viscosity was significant on the delivered volume after the first and the 50^{th} injection ($p < 0.05$) for different reciprocating frequencies. However, the effect of reciprocating frequency on volume delivered after the first and the 50^{th} injection was insignificant ($p > 0.05$) for each liquid used in the study. It should be noted that the apparent viscosity used for statistical analysis was for shear rates in the range $10^{-4} - 10^{-2}\ s^{-1}$.

3.3 Ex vivo injections

To ascertain if the results presented here can be translated to living tissue, we performed ex vivo injections on excised human skin. Newtonian fluids (DI water and 80% glycerol) were used for injections which lasted 2 seconds at the frequencies used for injections into gel (Fig. 6a). Although as earlier mentioned, the exposure of needles was set to a depth of 1 mm, the measured depth of deposited ink observed from the excised cross section was typically much less (0.32 ± 0.04 mm).

Using digital image processing on cross section images, we measured the area (mm^2) covered by the ink after injections. Figure 6 shows the estimated cross sectional area (A_p) of ink infusion inside skin as a function of reciprocating frequency for DI water and 80% glycerol. A_p increased with increasing f, with higher delivery for the less viscous fluid (DI water) showing that higher f and lower μ are desirable to deliver more fluid via tattoo injections. Using ANOVA analysis, the effect of viscosity and frequency was significant on the projected area for Newtonian fluids used here ($p < 0.05$ for both parameters).

4 Conclusions and outlook

A preliminary study of the efficacy of the tattooing process for ID drug delivery is undertaken. The major effects outlined are from the physical properties of the fluid. The effect of viscosity of fluids plays a vital role in fluid infusion into the cavities created, but the effect of reciprocating frequency was insignificant. We highlight an inverse relation between volume delivered, V_o and viscosity of the fluid used that is seen in the

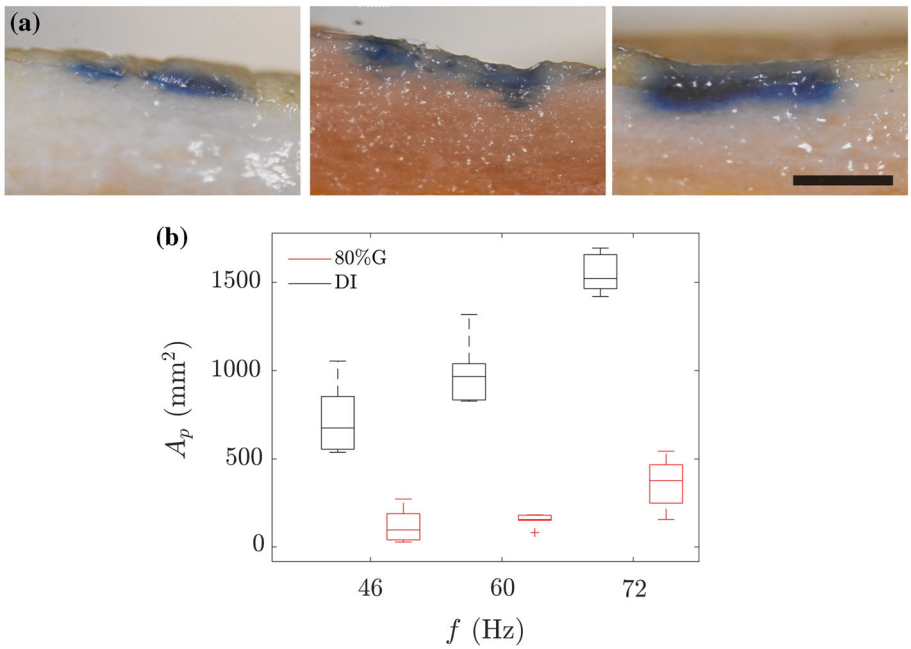

Fig. 6 **a** Cross section of excised human skin injected with 80% glycerol at 46 Hz, 60 Hz and 72 Hz (L-R), (Scale bar represents 1 mm) **b** covered Area (side view) (A_p) plotted against reciprocating frequency (f) for DI water and 80% glycerol

Newtonian case but more complex in the Non-Newtonian case. We also posit two possible ways to explain the nature of the capillary imbibition into the cavities in the more complex non-Newtonian fluids although it is yet to be quantitatively proven. Furthermore, we have shown that multiple punctures are indeed required to deliver more fluid into the substrate (a consequence of lubrication of the needles by the injectate) but limited by the saturation of the capacity of the cavity created by puncturing. Ultimately, our study, albeit preliminary in nature, presents an interesting baseline for any future research that may be concerned with the physics of this process. Moreover, more detailed experiments to verify and quantify the infusion mechanism in order to better understand the role of fluid rheology/viscosity can yet be done. Likewise, more refined ex vivo experiments to estimate volume can be pursued. A deeper understanding of this process could in theory provide the basis for optimization of the tattoo procedure in any aspect that it may be used. In addition we recommend that future mechanistic studies focus on incorporating more realistic application of tattooing whereby the needle head is translated across the surface. These aspects are the subject of our ongoing/future studies.

Supplementary Information The online version contains supplementary material available at https://doi.org/10.1007/s12650-021-00816-5.

Acknowledgements J.M. acknowledges funding support through NSF (CAREER Award No. 1749382).

Author Contributions Conceptualization, J.M.; Methodology, J.M. and I.L.; Experiments, I.L.; Data Analysis, I.L. and P.R.; Writing – Original Draft, I.L. and P.R.; Writing – Review and Editing, J.M., I.L. and P.R.; Funding Acquisition, J.M.

Declarations

Conflict of interest The authors declare that they have no conflict of interest.

References

Friedman R, Antoine D, Talamo S, Reimer PJ, Taylor JH, Wills B, Mannino MA (2018) Natural mummies from predynastic egypt reveal the worlds earliest figural tattoos. J Archaeol Sci 92:116–125
Petersen H, Roth K (2016) To Tattoo or not to Tattoo: Vom Pigment zum Portrat. Chemie in Unserer Zeit 50(1):44–66
Kluger N, Koljonen V (2012) Tattoos, inks, and cancer. Lancet Oncol 13(4):e161–e168

Sato Y, Ohshima T, Kondo T (1999) Regulatory role of endogenous interleukin-10 in cutaneous inflammatory response of murine wound healing. Biochem Biophys Res Commun 265(1):194–199
Jang D, Kim D, Moon J (2009) Influence of fluid physical properties on ink-jet printability. Langmuir 25(5):2629–2635
Mohammed AJ, AlAwaidy S, Bawikar S, Kurup PJ, Elamir E, Shaban MMA, Sharif SM, van der Avoort HGAM, Pallansch MA, Malankar P et al (2010) Fractional doses of inactivated poliovirus vaccine in oman. N Engl J Med 362(25):2351–2359
Belshe RB, Newman FK, Cannon J, Duane C, Treanor J, Van Hoecke C, Howe BJ, Dubin G (2004) Serum antibody responses after intradermal vaccination against influenza. N Engl J Med 351(22):2286–2294
Bryan JP, Sjogren MH, Perine PL, Legters LJ (1992) Low-dose intradermal and intramuscular vaccination against hepatitis b. Clin Infect Dis 14(3):697–707
Rohilla P, Marston J (2020) Feasibility of laser induced jets in needle free jet injections. Int J Pharm 589:119714
Weniger BG, Papania MJ (2013) Alternative vaccine delivery methods. Vaccines, 1200
Yuen C, Liu Q (2015) Hollow agarose microneedle with silver coating for intradermal surface-enhanced raman measurements: a skin-mimicking phantom study. J Biomed Opt 20(6):061102
Peng S, Monie A, Kang TH, Hung C-F, Roden R, Wu TC (2010) Efficient delivery of dna vaccines using human papillomavirus pseudovirions. Gene Ther 17(12):1453–1464
Chen D, Endres R, Maa Y-F, Kensil CR, Whitaker-Dowling P, Trichel A, Youngner JS, Payne LG (2003) Epidermal powder immunization of mice and monkeys with an influenza vaccine. Vaccine 21(21–22):2830–2836
Lengsfeld CS, Anchordoquy TJ (2002) Shear-induced degradation of plasmid dna. J Pharm Sci 91(7):1581–1589
Quaak SGL, van den Berg JH, Oosterhuis K, Beijnen JH, Haanen JBAG, Nuijen B (2009) Dna tattoo vaccination: effect on plasmid purity and transfection efficiency of different topoisoforms. J Control Release 139(2):153–159
Shio MT, Paquet M, Martel C, Bosschaerts T, Stienstra S, Olivier M, Fortin A (2014) Drug delivery by tattooing to treat cutaneous leishmaniasis. Sci Rep 4(1):1–7
Potthoff A, Schwannecke S, Nabi G, Hoffmann D, Grunwald T, Wildner O, Brockmeyer NH, Überla K, Tenbusch M (2009) Immunogenicity and efficacy of intradermal tattoo immunization with adenoviral vector vaccines. Vaccine 27(21):2768–2774
Gopee NV, Cui Y, Olson G, Warbritton AR, Miller BJ, Couch LH, Wamer WG, Howard PC (2005) Response of mouse skin to tattooing: use of skh-1 mice as a surrogate model for human tattooing. Toxicol Appl Pharmacol 209(2):145–158
Cu Katharina, Bansal Ruchi, Mitragotri Samir, Rivas David Fernandez (2019) Delivery strategies for skin: comparison of nanoliter jets, needles and topical solutions. Annals of Biomedical Engineering, 1–12
Gálvez LO, Pérez MB, Rivas DF (2019) High speed imaging of solid needle and liquid micro-jet injections. J Appl Phys 125(14):144504
Cross MM (1965) Rheology of non-newtonian fluids: a new flow equation for pseudoplastic systems. J Colloid Sci 20(5):417–437
Rohilla P, Marston JO (2019) In-vitro studies of jet injections. Int J Pharm 568:118503
Delalleau A, Josse G, Lagarde J-M, Zahouani H, Bergheau J-M (2006) Characterization of the mechanical properties of skin by inverse analysis combined with the indentation test. J Biomech 39(9):1603–1610
Pailler-Mattei C, Bec S, Zahouani H (2008) In vivo measurements of the elastic mechanical properties of human skin by indentation tests. Med Eng Phys 30(5):599–606
Andersson J, Ström A, Gebäck T, Larsson A (2017) Dynamics of capillary transport in semi-solid channels. Soft Matter 13(14):2562–2570
Prakash M, Quéré D, Bush JWM (2008) Surface tension transport of prey by feeding shorebirds: the capillary ratchet. Science 320(5878):931–934